IEEE Access
Multidisciplinary ⋮ Rapid Review ⋮ Open Access Journal

Received December 26, 2019, accepted January 14, 2020, date of publication February 13, 2020, date of current version March 2, 2020.

Digital Object Identifier 10.1109/ACCESS.2020.2973816

A Diagnosis of Grounding Grid Corrosion Defects Based on Branch Voltage Disturbance

MANLING DONG[1], ZHEN SHI[2], XING LI[3], GUANGQI SHAO[2], FAN YANG[3], DEGUI YAO[1], AND KE ZHANG[1]

[1]State Grid Henan Electric Power Corporation Research Institute, Zhengzhou 450052, China
[2]College of Electrical Engineering, Guangxi University, Nanning 400044, China
[3]State Key Laboratory of Power Transmission Equipment and System Security and New Technology, Chongqing University, Chongqing 400044, China

Corresponding author: Zhen Shi (eee0619@sina.com)

This work was supported in part by the National Natural Science Foundation of China under Grant 51907034, Grant 51867003, and Grant 61473272, in part by the General Ministry of Science and Technology Project of State Grid Corporation of China under Grant 5200-201924068A-0-0-00, in part by the Natural Science Foundation of Guangxi under Grant 2018JJB160056, Grant 2018JJB160064, and Grant 2018JJA160176, in part by the Basic Ability Promotion Project for Yong Teachers in Universities of Guangxi under Grant 2019KY0046 and Grant 2019KY0022, in part by the Guangxi Thousand Backbone Teachers Training Program, in part by the Boshike Award Scheme for Young Innovative Talents, and in part by the Guangxi Bagui Young Scholars Special Funding.

ABSTRACT The grounding grid is the cornerstone for maintaining the safe operation of the power system. The grounding network acts as a concealed project, and its invisible characteristics make the defects difficult to be detected, which causes major safety hazards in the system. Thus accurate diagnosis of grounding grid corrosion is vital in electrical engineering. A diagnosis method for grounding grid corrosion based on branch voltage disturbance is proposed in this paper, which can judge the location and degree of corrosion through branch voltage disturbance before and after corrosion. Firstly, the sensitivity of branch voltage to branch resistance of the grounding grid is analyzed. Secondly, a diagnostic model based on branch voltage disturbance is established, and the corresponding regularity between peak voltage disturbance and the corrosion state of the grounding grid branch is developed. Finally, it is verified by experiments that this method can effectively diagnose the corrosion of the grounding grid.

INDEX TERMS Grounding grid, corrosion, defect diagnosis, voltage disturbance.

I. INTRODUCTION

The grounding grid provides a reference potential for the substation and discharges dangerous currents caused by lightning and short circuit of the power system to ensure the safety and stability of the power system [1]–[4]. However, due to the non-standard construction and poor working environment of the grounding grid, the grounding grid is susceptible to electrochemical and biological corrosion [5]–[7]. The corrosion makes grounding performance unable to meet the requirements for safe operation of the power system, posing a threat to the safety of the power system and personnel [8]–[10]. The large grounding grid is buried in the soil about 0.8m deep underground, which is difficult to be excavated and replaced [11]. Therefore, it is of great engineering significance to predict the corrosion defects of the grounding grid through the accessible information above the ground surface to guide the operation and maintenance [12]–[15].

The associate editor coordinating the review of this manuscript and approving it for publication was Baoping Cai.

In the research of grounding grids, the optimal design and grounding performance of grounding grids are generally studied abroad [16], [17]. In China, many scholars are committed to the study of corrosion diagnosis, because the corrosion of the old substation grounding grid is common, and the degree of corrosion is relatively serious. Therefore, based on the electromagnetic field theory and electrical network theory, some diagnostic methods were proposed [18]. The basic idea of the former method is to inject a current into the grounding grid or excite the grounding grid with the coil current, measure the surface magnetic field, and reflect the corrosion through the magnetic field distribution [19], [20]. The magnetic field measured by this method has obvious collapse phenomenon at the breaking point of the grounding grid branch, which can diagnose the broken branch, but it is difficult to accurately diagnose the corrosion of the unbroken branch. For another method, each branch of the grounding grid is equivalent to a pure resistor, and a diagnostic model could be established by using the electrical network theory for fault prediction [21], [22]. According to the Tellegen's

theorem, the relationship between the down lead port resistance and branch resistance was established in reference [23] to carry out corrosion diagnosis. Besides, sensitivity relationships between branch resistance, node voltage, and port voltage were established in the study [24]. However, the diagnosis effect of this method was not satisfactory—it directly used the node potential of the grounding grid to establish a corrosion diagnosis mathematical model, lacked deep extraction of the internal relationship between the node potential data and the corrosion state, and most of the established diagnosis mathematical models were non-linear and underdetermined, which need to be solved by the optimization algorithm [25], [26]. Based on the existing research foundation, this paper proposed a method to reflect the branch corrosion by the voltage disturbance of the grounding grid branch. The characteristic of branch voltage disturbance caused by branch resistance of the grounding grid was theoretically analyzed. After injecting a current to the grounding grid, a mapping relationship between the unit distance voltage disturbance and the corrosion state could be established based on the change of each branch voltage before and after the corrosion, which reflected the location of the corrosion branch and the severity of corrosion. Finally, experiments verified the feasibility of the method, and the method could accurately diagnose the corrosion fault of the grounding grid.

II. VOLTAGE DISTURBANCE CHARACTERISTICS OF GROUNDING NETWORK BRANCH

A. GROUNDING GRID MODEL

The grounding grid can be equivalent to a pure resistance network [27] by injecting a small direct current into the grounding grid and ignoring the soil stray current. An equivalent physical model of the grounding grid is shown in Fig. 1.

Based on the theory of the electrical network, the mathematical model of the grounding network can be expressed as

$$\boldsymbol{U}_{\mathrm{n}} = \boldsymbol{Y}_{\mathrm{n}}^{-1}\boldsymbol{I}_{\mathrm{n}} \tag{1}$$

$$\boldsymbol{U}_{\mathrm{b}} = \boldsymbol{A}^{\mathrm{T}}\boldsymbol{U}_{\mathrm{n}} = \boldsymbol{A}^{\mathrm{T}}\boldsymbol{Y}_{\mathrm{n}}^{-1}\boldsymbol{I}_{\mathrm{n}} \tag{2}$$

where $\boldsymbol{A}$ is the correlation matrix, $\boldsymbol{U_n}$ is the node voltage matrix, $\boldsymbol{U_b}$ is the branch voltage matrix, $\boldsymbol{I_n}$ is the node current matrix, and $\boldsymbol{Y_n}$ is the node admittance matrix.

B. ANALYSIS OF BRANCH VOLTAGE DISTURBANCE

For a resistor network, under the same excitation condition, the disturbance capability of branch resistance changes to each branch voltage is different. To reflect the disturbance of branch resistance to branch voltage, the branch voltage is fully differentiated.

$$\begin{aligned}\mathrm{d}\boldsymbol{U}_{\mathrm{b}} &= \sum_{i=1}^{\mathrm{b}} \frac{\partial\left(\boldsymbol{A}^{\mathrm{T}}\boldsymbol{Y}_{\mathrm{n}}^{-1}\boldsymbol{I}_{\mathrm{n}}\right)}{\partial R_i}\mathrm{d}R_i \\ &= \boldsymbol{A}^{\mathrm{T}}\sum_{i=1}^{\mathrm{b}}\left[\frac{\partial\left(\boldsymbol{Y}_{\mathrm{n}}^{-1}\right)}{\partial R_i}\boldsymbol{I}_{\mathrm{n}} + \boldsymbol{Y}_{\mathrm{n}}^{-1}\frac{\partial \boldsymbol{I}_{\mathrm{n}}}{\partial R_i}\right]\mathrm{d}R_i\end{aligned} \tag{3}$$

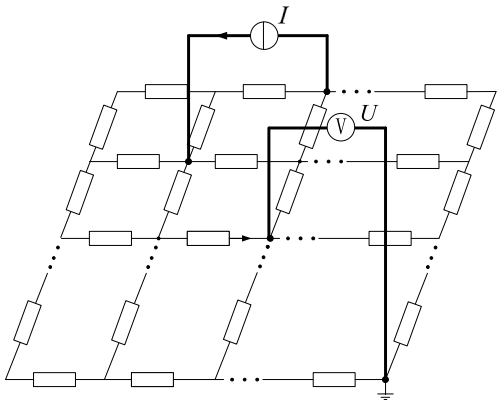

FIGURE 1. An equivalent physical model of the grounding grid.

Since only the current source is excited, the node current $\boldsymbol{I_n}$ is independent of the branch resistance R_i, so

$$\mathrm{d}\boldsymbol{U}_{\mathrm{b}} = \boldsymbol{A}^{\mathrm{T}}\sum_{i=1}^{\mathrm{b}}\left[\frac{\partial\left(\boldsymbol{Y}_{\mathrm{n}}^{-1}\right)}{\partial R_i}\boldsymbol{I}_{\mathrm{n}}\right]\mathrm{d}R_i \tag{4}$$

By using matrix analysis theory, the equation can be expressed as:

$$\frac{\partial\left(\boldsymbol{Y}_{\mathrm{n}}^{-1}\right)}{\partial R_i} = -\boldsymbol{Y}_{\mathrm{n}}^{-1}\boldsymbol{A}\frac{\partial \boldsymbol{R}^{-1}}{\partial R_i}\boldsymbol{A}^{\mathrm{T}}\boldsymbol{Y}_{\mathrm{n}}^{-1} \tag{5}$$

Combining equations (1), (4) and (5), equation (6) is obtained and shown below.

$$\mathrm{d}\boldsymbol{U}_{\mathrm{b}} = \boldsymbol{A}^{\mathrm{T}}\sum_{i=1}^{\mathrm{b}}\left[-\boldsymbol{Y}_{\mathrm{n}}^{-1}\boldsymbol{A}\frac{\partial \boldsymbol{R}^{-1}}{\partial R_i}\boldsymbol{A}^{\mathrm{T}}\boldsymbol{U}_{\mathrm{n}}\right]\mathrm{d}R_i \tag{6}$$

where

$$\frac{\partial \boldsymbol{R}^{-1}}{\partial R_i} = \begin{bmatrix} 0 & 0 & 0 & \cdots & 0 \\ 0 & 0 & \vdots & 0 & 0 \\ 0 & \cdots & -\dfrac{1}{R_i^2} & \cdots & 0 \\ 0 & 0 & \vdots & 0 & 0 \\ 0 & 0 & 0 & \cdots & 0 \end{bmatrix} \tag{7}$$

$\boldsymbol{S}$ is defined as the disturbance matrix of the branch resistance to the branch voltage,

$$\mathrm{d}\boldsymbol{U}_{\mathrm{b}} = \boldsymbol{S}\,\mathrm{d}\boldsymbol{R} \tag{8}$$

where

$$\boldsymbol{S} = \begin{bmatrix}\boldsymbol{S}(:,1) & \boldsymbol{S}(:,2) & \cdots & \boldsymbol{S}(:,\mathrm{b})\end{bmatrix}_{(\mathrm{n}-1)\times\mathrm{b}} \tag{9}$$

$$\boldsymbol{S}(:,i) = \boldsymbol{A}^{\mathrm{T}}\left[-\boldsymbol{Y}_{\mathrm{n}}^{-1}\boldsymbol{A}\frac{\partial \boldsymbol{R}^{-1}}{\partial R_i}\boldsymbol{A}^{\mathrm{T}}\boldsymbol{U}_{\mathrm{n}}\right] \tag{10}$$

where S_{ij} represents the disturbance coefficient of the resistance of the j branch to the voltage of the i branch. The absolute value of the disturbance coefficient is generally used to characterize the disturbance capability.

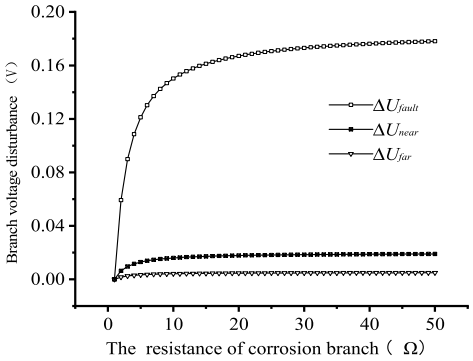

FIGURE 2. The change of different branch voltages along with the resistance of corrosion branch.

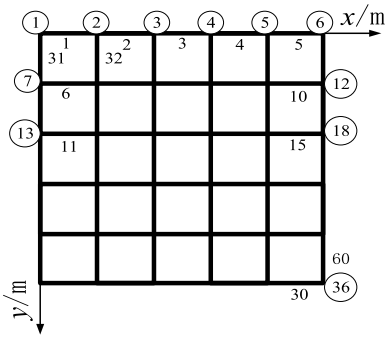

FIGURE 3. The grounding grid diagnosis model.

By analyzing the absolute value of $\boldsymbol{S}$ elements, it is found that the diagonal elements have obvious dominant phenomena in each column, indicating that the resistance of each branch has the highest voltage perturbation capability. Therefore, if one branch of the grounding grid is corroded and the resistance becomes large, the variation value of the branch voltage U_{fault} will be significantly larger than other branches. Reasonable selection of the current excitation injection point can extract the corrosion state information of the grounding network branch from the disturbance of branch voltage.

To study the variation of the corrosion branch voltage with the corrosion degree, a branch is arbitrarily selected as the corrosion branch from a 5*5 resistor grid with 50 branches, and its resistance range is set to $1 \sim 20\Omega$ (the resistance value of a normal branch is 1Ω). Then, the branch voltage is calculated. Voltage changes of the corrosion branch(ΔU_{fault}), the branch near the corrosion branch(ΔU_{near}), and the branch far from the corrosion branch (ΔU_{far}) are shown in Fig. 2.

As can be seen from Fig. 2, the variation of branch voltage before and after corrosion can be approximated as follows:

$$\Delta U_{fault} > \Delta U_{near} \geq \Delta U_{far} \tag{11}$$

After the grounding grid is corroded, the voltage change of the corroded branch is more obvious than that of other branches, which reflects the position and corrosion degree of the corroded branch.

III. THE DIAGNOSIS METHOD OF THE GROUNDING GRID CORROSION

A. DIAGNOSTIC PRINCIPLE

For a grounding grid with complicated branch structures, when corrosion occurs, the proportion of the far-corrosion branch is large, and the law of equation (11) is more obvious. The voltage change of the corrosion branch is larger than that of the other branches, so this information can be used as an indirect feature to reflect the corrosion state.

For an actual grounding grid, the length of each branch is not uniform. To eliminate the interference of different initial resistances of branches with various lengths to the voltage variation, the voltage variation value per unit distance (i.e. voltage disturbance) is used as a direct feature to reflect the corrosion state of the grounding grid, which is defined below:

$$\lambda = \frac{|\Delta(U_i - U_j)|}{l_{ij}} = \frac{\left|(U_i' - U_j') - (U_i - U_j)\right|}{l_{ij}} \tag{12}$$

where U_i, U_j, U_i' and U_j' are the potentials of adjacent nodes i and j of the grounding grid before and after corrosion under the same excitation, l_{ij} is the distance between i and j (dimensionless value in meters).

The potential difference between adjacent nodes is the voltage on each branch.

$$\lambda = \frac{|\Delta(U_i - U_j)|}{l_{ij}} = \frac{\left|U_{ij}' - U_{ij}\right|}{l_{ij}} = \frac{|\Delta U_{ij}|}{l_{ij}} \tag{13}$$

When the grounding grid is not corroded, the branch resistance is proportional to the length of the branch (i.e. $R_{ij} \propto l_{ij}$).

$$\lambda = \frac{|\Delta U_{ij}|}{l_{ij}} \propto \frac{|\Delta U_{ij}|}{R_{ij}} \propto |\Delta U_{ij}| \tag{14}$$

where R_{ij} is the initial resistance of branch ij before corrosion.

B. CORROSION LOCATION AND EVALUATION

1) NODE POTENTIAL INTERPOLATION

To facilitate analysis, a coordinate grid model of the grounding grid is established according to the actual grounding grid structure. Fig. 3 shows the diagnostic model of the grounding grid with the grid size of 1 m × 1 m, and it includes 60 branches. The numbering rules for nodes and branches are first from left to right and then from top to bottom.

According to the diagnosis principle, it is necessary to obtain as many node potentials as possible to calculate the voltage disturbance. For the grounding grid of the actual substation, there is no guarantee that there is sufficient down conductor to collect the potential. Therefore, the potential of the unknown node is obtained by using the Lagrangian linear interpolation.

As shown in Fig. 4, the potential of the node 5 is obtained by interpolation of the node 2, 4, 6, and 8. Formulas for calculating the interpolation are shown as follows:

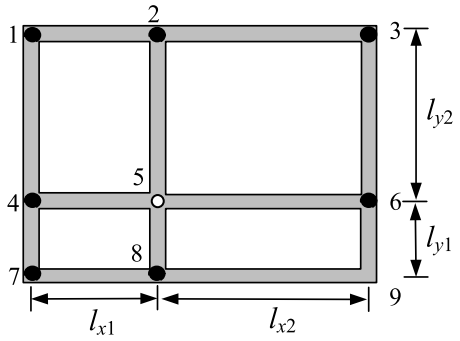

FIGURE 4. Interpolation for the unknown node potential.

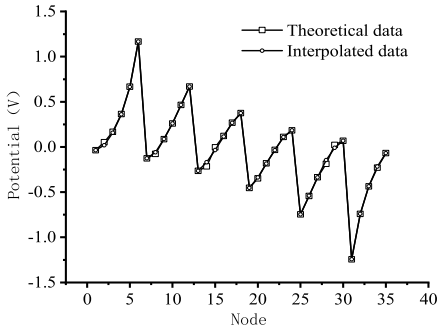

FIGURE 5. The comparison between the theoretical calculation and interpolation calculation.

Horizontal interpolation U_{5x}

$$U_{5x} = \left[\frac{l_{x2}}{l_{x1}}(U_4 - U_6) + U_6\right] \tag{15}$$

Longitudinal interpolation U_{5y}

$$U_{s_y} = \left[\frac{l_{y1}}{l_{y2}}(U_2 - U_8) + U_8\right] \tag{16}$$

To improve the interpolation accuracy, the average of the horizontal and longitudinal interpolation is taken as the interpolation result.

$$U_5 = \frac{\left[\frac{l_{x2}}{l_{x1}}(U_4 - U_6) + U_6\right] + \left[\frac{l_{y1}}{l_{y2}}(U_2 - U_8) + U_8\right]}{2} \tag{17}$$

For the model in Fig. 3, a current of 1A is injected from node 1, and the current flows from node 31, and the resistance of each branch is set to 1. The comparison of the node potential calculated by theoretical calculation and interpolation calculation is shown in Fig. 5. The result shows that the difference between the theoretical data and interpolated data is small—the potential value obtained by the interpolation method has high precision.

2) EVALUATION OF CORROSION DEGREE

The magnitude change of the voltage disturbance has a corresponding relationship with the resistance of the corrosion branch so that the degree of corrosion of the grounding grid can be evaluated. It can be known from the branch voltage perturbation law that the value of the voltage disturbance increases as the resistance becomes larger.

$$\lambda = I\left(aR^b + c\right) \tag{18}$$

where λ is the voltage disturbance, R is the branch resistance, I is the current injected into the grounding grid, a, b and c are fitting constants.

Taking branch 23 of the model in Fig. 3 as an example, a current of 1A is injected from node 6 and flows out from node 31. The initial resistance of each branch is 1Ω. The corrosion degree curve can be obtained by fitting the variation law of voltage disturbance, which is shown in Fig. 6.

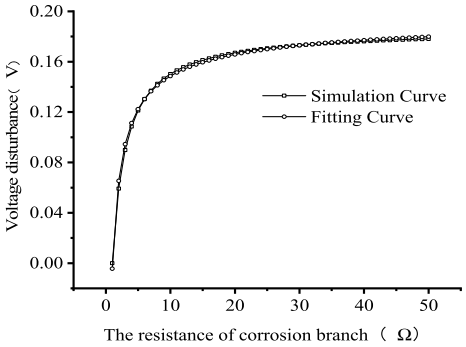

FIGURE 6. The fitting curve on corrosion degree.

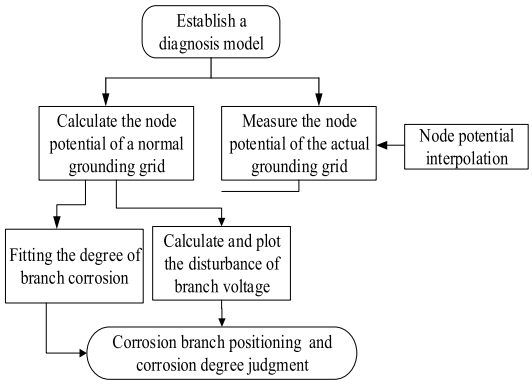

FIGURE 7. The process of the grounding grid diagnosis.

The functional equation of the fitting curve is

$$\lambda = -0.2031\mathrm{R}^{-0.6079} + 0.1987 \tag{19}$$

It can be seen that the power exponential function achieves a good fit of the corrosion law, and the fitness is R-square = 0.9998.

Then the corrosion degree formula of the branch is

$$\mathrm{R} = [(\lambda - 0.1987)/(-0.2031)]^{\frac{1}{-0.6079}} \tag{20}$$

The specific process for corrosion positioning and evaluation of the grounding grid is shown in Fig. 7. Firstly, a diagnostic model is established according to the structural parameters of the grounding grid, and the node potential of

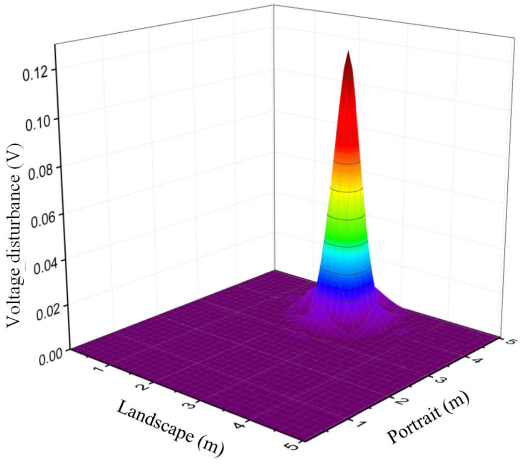

FIGURE 8. Simulation result of single corrosion fault.

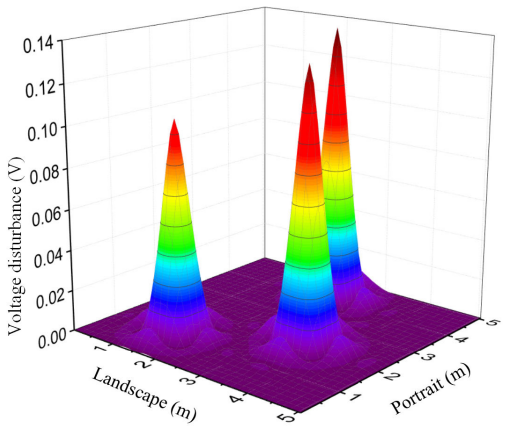

FIGURE 9. Simulation result of three corrosion faults.

the grounding grid before corrosion and the corrosion degree curve of the branch are obtained through theoretical calculation. Secondly, the node potential after corrosion is measured and interpolated under the same excitation. The voltage disturbance is calculated by using the potential data before and after corrosion, and it is presented in a three-dimensional graph. Finally, the corrosion state of the grounding grid can be diagnosed and evaluated by the peak position and size of the three-dimensional graph.

IV. EXPERIMENTAL ANALYSIS

A. SIMULATION EXPERIMENT

For the grounding grid model shown in Fig. 3, a corrosion diagnosis simulation experiment was carried out by using the voltage disturbance. The two diagonal nodes 6 and 31 of the grounding grid were selected as the injection and outflow points of the current source, and node 36 was the potential reference node. A current of 1A was injected, and the initial value of each branch resistance is set to 1Ω.

1) SINGLE CORROSION DIAGNOSIS

When a single corrosion fault occurs, the resistance of branch 23 was set to 5Ω, and the voltage disturbance of each branch was calculated. The result is shown in Fig. 8.

The peak coordinate of the diagnosis result is (2.5, 4) corresponding to the branch 23 in the diagnostic model. Thus, the positioning of the corrosion branch is accurately achieved. At the same time, the peak value is substituted into Equation (20) to calculate the resistance of the corrosion branch that is 4.86Ω. The diagnostic error is only 2.8%, which enables accurate diagnosis of corrosion faults.

2) MULTI-CORROSION DIAGNOSIS

To simulate more complex corrosion conditions, three corrosion branches were established with different degrees of corrosion. The resistances of branch 23 and branch 7 were set to 5Ω and 3Ω, and that of branch 14 was set to 8Ω. The simulation result is shown in Fig. 9.

The coordinates and values corresponding to the peaks can be found in Fig. 9. Combined with the diagnosis model and the corrosion curve, resistances of three corrosion branches are 4.82Ω, 2.74Ω and 6.98Ω. Therefore, the fault location and the approximate judgment of the corrosion branch resistance can also be realized to meet the diagnostic requirements in the multi-corrosion diagnosis.

B. ANALOG GROUNDING GRID EXPERIMENT

The grid side length of the actual grounding grid was about 5m, and the branch resistance was about tens of milliohms. The laboratory used the same flat steel material of the grounding grid to weld the scaled analog grounding grid, and its grid side length was 1m. In the simulated grounding grid, the corrosion of the grounding grid was simulated by crimping two pieces of flat steel, and the resistance increased about 6 times as much as that of the normal branch. In the experiment, a current of 6A was injected through diagonal nodes 1 and 32 of the grounding grid, and a high-precision potential acquisition device FLUKE8845A was used to acquire the potential on the down conductor, and the potential value of the node without the down conductor was obtained through interpolation. The schematic diagram of the analog grounding grid and the experimental site diagram are shown in Fig. 10.

The voltage disturbance distribution of the analog grounding grid obtained by calculation is shown in Fig. 11. It can be determined that the corrosion branch of the grounding grid is covered by nodes 1-16. Basically, branch 1 is a corrosion branch, and the smaller peak around branch 1 may be a pseudo fault or a real fault with less corrosion.

On the basis of the first diagnosis, it was necessary to further narrow the corrosion branch range and eliminate false faults to achieve precise positioning. Thus, a current was injected from node 1, and was drawn from node 16. The potential of the grounding grid was measured for voltage disturbance calculation. The result is shown in Fig. 12.

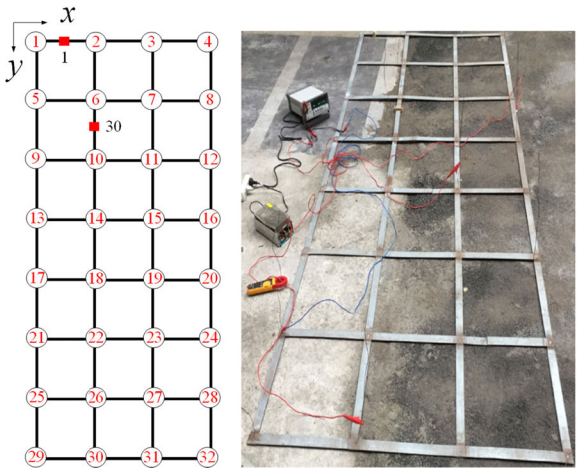

FIGURE 10. Grounding grid simulation and testing.

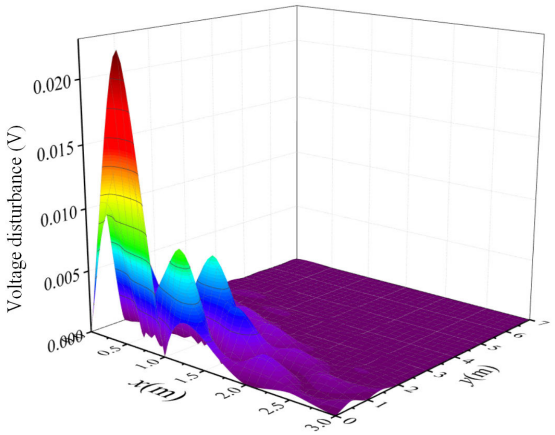

FIGURE 11. Diagnosis result of a single fault.

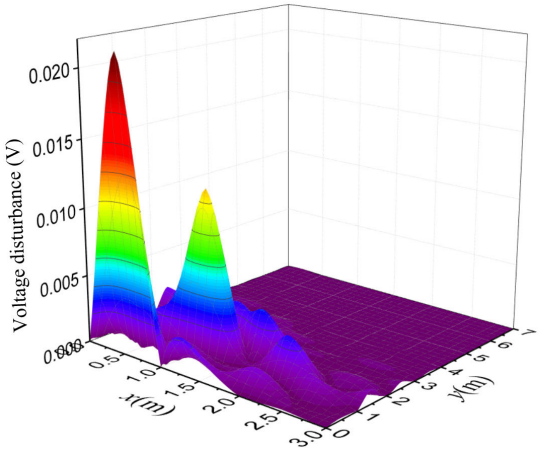

FIGURE 12. Diagnosis result of double faults.

According to the results of the above two diagnoses, there are two distinct peaks in the voltage disturbance distribution, and positions of these peaks correspond to branch 1 and branch 30 in the simulated grounding grid. This result is consistent with the corrosion point of the preset value in the simulated grounding grid, and the resistance of the corrosion branch is about 4-6 times that of the normal branch. Therefore, the diagnose realizes the accurate positioning of the corrosion branch of the grounding grid and the rough judgment of the corrosion degree.

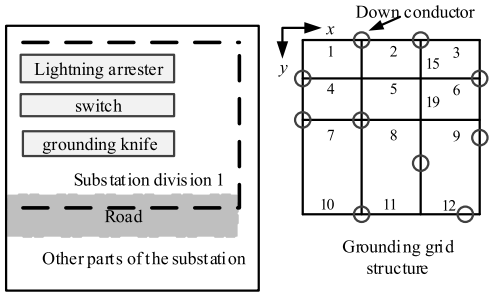

FIGURE 13. The block of substation and the grounding grid.

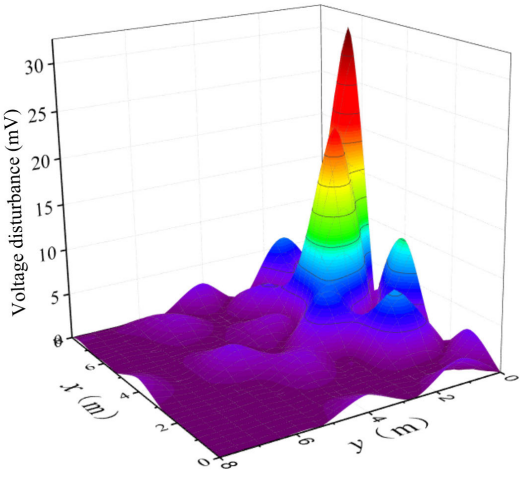

FIGURE 14. Voltage disturbance distribution of the grounding grid block.

C. SUBSTATION FIELD EXPERIMENT

In order to verify the effect of voltage disturbance on corrosion diagnosis of the grounding grid in the actual substation, a small waste substation partition was selected in central China for on-site diagnosis experiments. The selected grounding grid partition was approximately square, and its side length was about 8m. Fig.13 presents the structural schematic diagram of substation division 1 and the grounding grid.

We injected a DC current of 1A into the grounding grid, collected the potential data of the node through the grounding grid, and obtained potential interpolation to calculate the disturbance voltage of branches. The distribution result is shown in Fig 14.

Through on-site excavation, it was found that there were two branches with serious corrosion and poor welding at the corner of the grounding grid branch under the isolating switch. The specific location is shown in Fig. 15, which was close to the diagnostic result position of the voltage

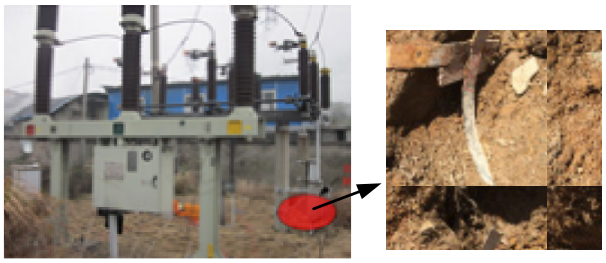

FIGURE 15. The location of corroded grounding grid branch.

disturbance distribution diagram. Thus, the correctness and practical effectiveness of the method were verified.

V. CONCLUSION

A new method of the grounding grid corrosion diagnosis based on branch voltage disturbance is proposed to overcome the shortcomings of the low internal information utilization rate of down-conductor potential data set and poor diagnosis effect of the established model in the grounding grid corrosion diagnosis. Through theoretical analysis and experimental verification, the following conclusions are drawn:

- Before and after corrosion of the grounding grid, the voltage disturbance caused by the increased resistance of corrosion branch is much larger than that of other branches.
- In the node potential data acquisition by measuring the grounding grid down-conductor, and the collected data is limited by the number of down-conductors. The reconstruction of the unknown node potential data can be performed by using the Lagrangian linear interpolation, which has high precision.
- Branch voltage disturbance of the grounding grid is calculated in this paper. From the distribution diagram, the corrosion branch and the corrosion degree of the grounding grid can be accurately located and evaluated through the position and value of the peak.

REFERENCES

[1] C. Yu, Z. Fu, G. Wu, L. Zhou, X. Zhu, and M. Bao, "Configuration detection of substation grounding grid using transient electromagnetic method," *IEEE Trans. Ind. Electron.*, vol. 64, no. 8, pp. 6475–6483, Aug. 2017.

[2] P. Liu and C. Huang, "Detecting single-phase-to-ground fault event and identifying faulty feeder in neutral ineffectively grounded distribution system," *IEEE Trans. Power Del.*, vol. 33, no. 5, pp. 2265–2273, Oct. 2018.

[3] B. Zhang, Z. Zhao, X. Cui, and L. Li, "Diagnosis of breaks in substation's grounding grid by using the electromagnetic method," *IEEE Trans. Magn.*, vol. 38, no. 2, pp. 473–476, Mar. 2002.

[4] B. Li, X. Ren, and B. Li, "Study on the charge transfer criterion for the pole-to-ground fault in DC distribution networks," *IEEE Access*, vol. 7, pp. 102386–102396, 2019.

[5] Y. Qiu, S. Thomas, D. Fabijanic, A. Barlow, H. Fraser, and N. Birbilis, "Electrochemical and corrosion properties of AlxCoCrFeNiTiy high entropy alloys," *Mater. Des.*, vol. 170, no. 107698, May 2019.

[6] L. Feng, A. Yan, Y. Meng, and J. Hou, "Investigation on corrosion of yttrium-doped magnesium-based sacrificial anode in ground grid protection," *J. Rare Earths*, vol. 28, pp. 389–392, Dec. 2010.

[7] B. W. Liu, H. Z. Ma, and H. H. Xu, "Single-phase-to-ground fault detection with distributed parameters analysis in non-direct grounded systems," *CSEE J. Power Energy Syst.*, vol. 5, no. 1, pp. 139–147, Mar. 2019.

[8] Z. Fu, X. Wang, Q. Wang, X. Xu, N. Fu, and S. Qin, "Advances and challenges of corrosion and topology detection of grounding grid," *Appl. Sci.*, vol. 9, no. 11, p. 2290, Jun. 2019.

[9] Y. Wang, Q. Xu, M. Liu, and J. Zheng, "A novel system operation mode with flexible bus type selection method in DC power systems," *Int. J. Elect. Power Energy Syst.*, vol. 103, pp. 1–11, Dec. 2018.

[10] Y. Xue, X. Chen, H. Song, and B. Xu, "Resonance analysis and faulty feeder identification of high-impedance faults in a resonant grounding system," *IEEE Trans. Power Del.*, vol. 32, no. 3, pp. 1545–1555, Jun. 2017.

[11] Y. J. Li, X. L. Meng, and X. H. Song, "Application of signal processing and analysis in detecting single line-to-ground (SLG) fault location in high-impedance grounded distribution network," *IET Gener., Transmiss. Distrib.*, vol. 10, no. 2, pp. 382–389, Feb. 2016.

[12] Z. He, H. Hu, W. Huang, Y. Pan, X. Li, and J. Yang, "A method of defect diagnosis for integrated grounding system in high-speed railway," *IEEE Trans. Ind. Appl.*, vol. 51, no. 6, pp. 5139–5148, Nov. 2015.

[13] Y. Zhang, X. Li, H. Zheng, H. Yao, J. Liu, C. Zhang, H. Peng, and J. Jiao, "A fault diagnosis model of power transformers based on dissolved gas analysis features selection and improved krill herd algorithm optimized support vector machine," *IEEE Access*, vol. 7, pp. 102803–102811, 2019.

[14] C. Yu, Z. Fu, Q. Wang, H.-M. Tai, and S. Qin, "A novel method for fault diagnosis of grounding grids," *IEEE Trans. Ind. Appl.*, vol. 51, no. 6, pp. 5182–5188, Nov. 2015.

[15] H. Wang, G. Tang, Z. He, and J. Yang, "Efficient grounding for modular multilevel HVDC converters (MMC) on the AC side," *IEEE Trans. Power Del.*, vol. 29, no. 3, pp. 1262–1272, Jun. 2014.

[16] H. Hu, R. Luo, M. Fang, S. Zeng, and F. Hu, "A new optimization design for grounding grid," *Int. J. Elect. Power Energy Syst.*, vol. 108, pp. 61–71, Jun. 2019.

[17] E.-S.-M. El-Refaie, S. E. Elmasry, M. K. A. Elrahman, and M. H. Abdo, "Achievement of the best design for unequally spaced grounding grids," *Ain Shams Eng. J.*, vol. 6, no. 1, pp. 171–179, Mar. 2015.

[18] H. Jouybari-Moghaddam, T. S. Sidhu, M. R. D. Zadeh, and P. P. Parikh, "Shunt capacitor banks online monitoring using a superimposed reactance method," *IEEE Trans. Smart Grid*, vol. 9, no. 6, pp. 5554–5563, Nov. 2018.

[19] X. Li, C. Li, X. Zhao, X. Du, X. Nie, Y. Xiong, J. Zhao, J. Sheng, Y. Wang, M. Zhang, and W. Yuan, "Study on two different charging methods for superconducting coils in persistent current mode," *Phys. C, Supercond. Appl.*, vol. 554, pp. 44–50, Nov. 2018.

[20] D. Qiu, Z. Y. Li, F. Gu, Z. Huang, A. Zhao, D. Hu, B. G. Wei, H. Huang, Z. Hong, K. Ryu, and Z. Jin, "Experiment study on an inductive superconducting fault current limiter using no-insulation coils," *Phys. C, Supercond. Appl.*, vol. 546, pp. 1–5, Mar. 2018.

[21] J. Liu, X. Fan, Y. Zhang, H. Zheng, and C. Zhang, "Condition prediction for oil-immersed cellulose insulation in field transformer using fitting fingerprint database," *IEEE Trans. Dielectr. Electr. Insul.*, vol. 27, no. 1, pp. 279–287, Feb. 2020, doi: 10.1109/TDEI.2019.008442.

[22] Y. Wang, Y. Huang, X. Zeng, G. Wei, J. Zhou, T. Fang, and H. Chen, "Faulty feeder detection of single phase-earth fault using grey relation degree in resonant grounding system," *IEEE Trans. Power Del.*, vol. 32, no. 1, pp. 55–61, Feb. 2017.

[23] L. Chunli, H. Wei, Y. Degui, Y. Fan, K. Xiaokuo, and W. Xiaoyu, "Topological measurement and characterization of substation grounding grids based on derivative method," *Int. J. Elect. Power Energy Syst.*, vol. 63, pp. 158–164, Dec. 2014.

[24] B. Anggoro and R. E. Yutadhia, "The grounding impedance characteristics of grid configuration," *Procedia Technol.*, vol. 11, pp. 1156–1162, Jan. 2013.

[25] J.-F. Bao, C. Li, W.-P. Shen, J.-C. Yao, and S.-M. Guu, "Approximate Gauss–Newton methods for solving underdetermined nonlinear least squares problems," *Appl. Numer. Math.*, vol. 111, pp. 92–110, Jan. 2017.

[26] P. Gaudreau, K. Hayami, Y. Aoki, H. Safouhi, and A. Konagaya, "Improvements to the cluster Newton method for underdetermined inverse problems," *J. Comput. Appl. Math.*, vol. 283, pp. 122–141, Aug. 2015.

[27] R. Prenc, D. Vučetić, and A. Cuculć, "High voltage shore connection in croatia: network configurations and formation of the connection point to the utility power grid," *Electr. Power Syst. Res.*, vol. 157, pp. 106–117, Apr. 2018.

MANLING DONG was born in Ningxia, China, in 1982. He received the M.S. and Ph.D. degrees in electrical engineering from the Huazhong University of Science and Technology, Wuhan, China, in 2008 and 2012, respectively. He is currently a Senior Engineer with the State Grid Henan Power Corporation Research Institute. His major research interests include the field of dielectric property of insulation systems for high voltage apparatus, online detection of insulation condition of high voltage apparatus, condition assessment, and insulation fault diagnosis for oil-paper insulation on high voltage apparatus.

ZHEN SHI was born in Guangxi, China, in 1987. He received the bachelor's degree in electrical engineering from the Shanghai University of Electric Power, in 2010, and the M.Sc. and Ph.D. degrees from the University of Strathclyde, U.K., in 2011 and 2018, respectively. He was studying abroad at the University of Strathclyde. In 2018, he joined the School of Electrical Engineering, Guangxi University, as a Postdoctoral Researcher. His research interests are mainly in the area of advanced partial discharge detection technologies, data analysis of partial discharge detection, and the online evaluation of electrical equipment insulation.

XING LI was born in 1991. He received the Ph.D. degree. He is currently with the State Grid Henan Power Corporation Research Institute. His research area is the electromagnetic imaging.

GUANGQI SHAO was born in Hubei, China, in 1993. He is currently pursuing the master's degree in electrical engineering with the College of Electrical Engineering, Guangxi University, China. His major research interests include status assessment and fault diagnosis of high voltage oil-paper insulated electrical equipment.

FAN YANG was born in 1980. He is currently a Doctoral Supervisor with Chongqing University. He is also interested in the areas of the numerical calculation of electromagnetic field and the evaluation of electromagnetic environment.

DEGUI YAO was born in 1971. He received the Ph.D. degree. He is currently a Professorate Senior Engineer with the State Grid Henan Power Corporation Research Institute. His research interest is the application of electromagnetic field.

KE ZHANG was born in 1970. He is currently a Senior Engineer with the State Grid Henan Power Corporation Research Institute. His research interest is the voltage disturbance influence on the power flow.